Composites: Part A 33 (2002) 1539–1547

composites
Part A: applied science and manufacturing

www.elsevier.com/locate/compositesa

Crack growth in discontinuous glass fibre reinforced polypropylene under dynamic and static loading conditions

A. Pegoretti*, T. Ricco[1]

Department of Materials Engineering, University of Trento, via Mesiano 77-38050 Trento, Italy

Received 5 January 2001; accepted 28 August 2002

Abstract

Crack propagation in single edge notched tensile specimens of isotactic polypropylene reinforced with short E-glass fibres has been investigated under both fatigue and creep loading conditions. Fatigue crack propagation (FCP) experiments have been performed at three different frequencies (0.1, 1, 10 Hz) and at a mean applied tensile load of 1200 N. Isothermal creep crack propagation (CCP) tests have been conducted under a constant tensile applied load of 1200 N at various temperatures in the range from 32 to 60 °C. Analysis of FCP data allowed an estimation of the pure fatigue and pure creep components of the crack velocity under the adopted cyclic loading conditions. Crack growth at low frequencies (0.1 and 1 Hz) is mainly associated with a non-isothermal creep process. At higher frequency (10 Hz), the pure fatigue contribution appeared more pronounced. Finally, the comparison of FCP and CCP as a function of the mean applied stress intensity factor confirmed the major contribution of creep crack growth during FCP process at low frequencies.

Keywords: A. Discontinuous reinforcement; A. Thermoplastic resin; B. Creep; B. Fatigue

1. Introduction

Due to its outstanding cost-to-performance ratio, low density, and ease of processing, isotactic polypropylene (iPP) has become one of the fastest developing thermoplastic polymers throughout the world [1]. A variety of performance characteristics can be achieved through modifications induced by molecular orientation [2], particulate filler addition [3], and reinforcement with short or long fibres [4]. In particular, short glass fibres are generally added into iPP in order to enhance its mechanical properties, such as stiffness and fracture resistance, without substantially impairing the good processability of the material. Moreover, the presence of short glass fibre in iPP reduces the propensity of this material to deform under fatigue and creep conditions, and hence helps to prevent failure in load-bearing applications. Fatigue and creep damage is generally associated with the initiation and propagation of cracks in the matrix and/or the destruction of the bonding at the fibre/matrix interface. For both neat polypropylene and its filled, short fibre and fibre mat reinforced composites, fractures mechanics approaches [5] have proven useful in providing a framework for characterization under service conditions and in defining safe operating conditions. Fatigue crack propagation (FCP) in short fibre reinforced iPP is generally characterised by the presence of a stable crack acceleration range [5–10] which can be well described by the following Paris-Erdogan relationship [11]

$$\left(\frac{\mathrm{d}a}{\mathrm{d}N}\right)_{\mathrm{F}} = A\Delta K^m \qquad (1)$$

where $(\mathrm{d}a/\mathrm{d}N)_{\mathrm{F}}$ is the fatigue crack growth rate per cycle, and ΔK is the difference between the maximum and minimum mode I, or opening mode, stress intensity factors in the fatigue cycle. A and m are pre-exponential and exponential constants, respectively. Eq. (1) can also be written as

$$\left(\frac{\mathrm{d}a}{\mathrm{d}t}\right)_{\mathrm{F}} = A'\Delta K^m \qquad (2)$$

where $(\mathrm{d}a/\mathrm{d}t)_{\mathrm{F}}$ is the fatigue crack growth velocity and $A' = A(1/f)$, f being the frequency of the fatigue load.

* Corresponding author. Tel.: +39-0461-882413; fax: +39-0461-881977.
E-mail address: alessandro.pegoretti@ing.unitn.it (A. Pegoretti).
[1] Current address: Department of Chemistry and Physics for Engineering and Materials, University of Brescia, via Valotti 9-25123 Brescia, Italy. (J. Ricco).

1359-835X/02/$ - see front matter © 2002 Published by Elsevier Science Ltd.
PII: S1359-835X(02)00112-4

For the creep crack propagation (CCP), a description similar to Eq. (2) is used [12]

$$\left(\frac{\mathrm{d}a}{\mathrm{d}t}\right)_{\mathrm{C}} = BK^n \tag{3}$$

where $(\mathrm{d}a/\mathrm{d}t)_{\mathrm{C}}$ is the creep crack growth velocity, K is the applied stress intensity factor under mode I loading condition, B and n are pre-exponential and exponential constants, respectively.

Under cycling loading at positive values of the mean load, the crack propagation rate in polymers is recognised to consist of the contributions of both fatigue and creep crack growth [8–10,13–17]. The analysis of FCP data obtained in a previous work on composites constituted by polypropylene reinforced with short glass fibres, showed that the crack propagation rate is determined mostly by viscoelastic creep processes at the crack tip, the role of fatigue appearing quite secondary [8–10]. However, during crack propagation the energy dissipation due to the dynamic load produces a temperature increase at the crack tip in these materials. Although it is difficult to measure the real extent of this temperature increase, experimental evidence of the non-isothermal character of the crack growth was found [9].

In the present work the role of fatigue and non-isothermal viscoelastic creep in the crack propagation within polypropylene/short-glass-fibre composites is investigated further. To achieve this, experiments of two types were conducted: FCP at a range of test frequencies and isothermal CCP at different temperatures.

2. Experimental details

2.1. Materials

Injection moulded square plaques (dimensions $127 \times 127 \times 2.7\ \mathrm{mm}^3$) of iPP reinforced with 10 wt% percent of short E-glass fibres were supplied by Montell Polyolefins SpA (Ferrara, Italy). The matrix was a commercial grade polypropylene with a melt flow index equal to 3.5 dg/min. The short E-glass fibres (Owens Coming R34B), with an average initial length of 4.5 mm and a diameter of 14 μm, were treated with a polypropylene compatible coating (Hercoprime HG 201). After compounding and injection-moulding the manufacturer evaluated an average fibre length of about 0.5–0.7 mm. Differential scanning calorimetry measurements performed on the composite indicated a melting temperature of 174 °C and a crystallinity content of about 62% [9]. For FCP and CCP tests, single edge notched tension (SENT) specimens, with dimensions as reported in Fig. 1, were machined from the injection-moulded plaques along the diagonal. An initial sharp notch of about 3 mm in length was introduced in the specimens by means of a razor blade attached to a CEAST saw cutter.

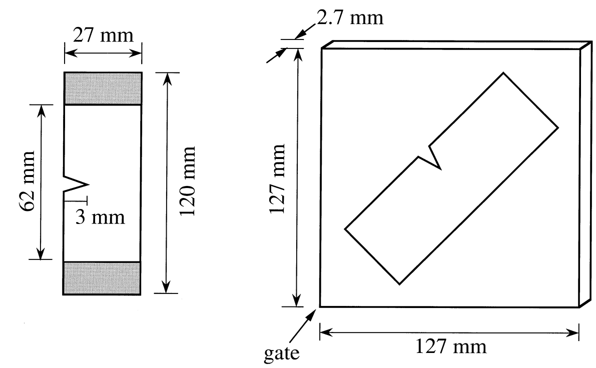

Fig. 1. Dimensions of polypropylene/glass SENT specimen and position with respect to the injection moulded plaque.

2.2. Fatigue crack propagation tests

Fatigue tests were performed at room temperature (normally 25 °C) under tension–tension sinusoidal load control, using a closed loop servohydraulic MTS 858 Mini Bionix testing machine. The mean load was 1200 N, the minimum to maximum load ratio was 0.4, and the cyclic frequencies were 0.1, 1, and 10 Hz. The crack length, a, was measured as a function of time, t, by a video-camera, a video-recorder, and an image analyser system. At least three specimens were tested for each experimental situation, and an average crack propagation rate, $\mathrm{d}a/\mathrm{d}t$, was obtained as the derivative of the best fitting third order polynomial curve. Parameters of best fitting polynomial function, $a(t) = At^3 + Bt^2 + Ct + D$, obtained by least squares regression of data, and the associated correlation coefficient, R, are reported in Table 1. Curves of $\mathrm{d}a/\mathrm{d}N$, where N is the number of cycles, were easily obtained by considering the frequency of the oscillating load. The stress intensity factor, K, at the crack tip was evaluated on the basis of the linear elastic fracture mechanics approach which is often used also to describe fracture and fatigue behaviour of non-linear and heterogeneous materials [15]. The specific equation for the stress intensity factor amplitude, ΔK, for SENT specimens is [18]

$$\Delta K = \frac{\Delta P}{BW}\sqrt{a}\left[1.99 - 0.41\frac{a}{W} + 18.7\left(\frac{a}{W}\right)^2 - 38.48\left(\frac{a}{W}\right)^3 + 53.85\left(\frac{a}{W}\right)^4\right] \tag{4}$$

where ΔP is the difference between the maximum and the minimum applied loads, B and W are the thickness and width of the specimens.

The temperature at the surface of the specimen near the crack tip region during FCP tests was monitored by an infrared sensing thermography camera (Hughes thermal video system TVS-300 Series). Scanning electron microscopy (SEM) was used to study the fracture surface of failed specimens. The microscope was a Cambridge

Table 1
Parameters of the best fitting third order polynomial function, $a(t) = At^3 + Bt^2 + Ct + D$, obtained by least squares regression of fatigue and creep crack propagation data. Correlation coefficient, r, is also reported

Test conditions	Specimen	A (mm/s^3)	B (mm/s^3)	C (mm/s)	D (mm)	Correlation coefficient, r
Fatigue crack propagation (FCP)						
$f = 0.1$ Hz	I	3.474×10^{-11}	-3.232×10^{-7}	2.291×10^{-3}	4.031	0.99498
	II	3.326×10^{-11}	-3.171×10^{-7}	2.251×10^{-3}	3.150	0.99535
	III	3.071×10^{-11}	-4.280×10^{-7}	2.468×10^{-3}	3.306	0.99808
f = 1 Hz	I	5.014×10^{-11}	-5.027×10^{-7}	2.335×10^{-3}	4.543	0.98858
	II	4.638×10^{-11}	-4.522×10^{-7}	2.842×10^{-3}	5.147	0.99666
	III	4.581×10^{-11}	-5.198×10^{-7}	2.834×10^{-3}	4.157	0.99565
f = 10 Hz	I	6.574×10^{-10}	-2.640×10^{-6}	5.816×10^{-3}	4.979	0.99819
	II	1.100×10^{-10}	-8.142×10^{-7}	2.946×10^{-3}	3.283	0.99774
	III	3.251×10^{-10}	-2.042×10^{-6}	5.129×10^{-3}	3.459	0.99519
Creep crack propagation (CCP)						
$T = 32$ °C		1.552×10^{-15}	-6.660×10^{-10}	1.373×10^{-4}	3.908	0.99730
$T = 35$ °C		9.775×10^{-15}	-2.100×10^{-9}	2.312×10^{-4}	4.495	0.99795
$T = 40$ °C		2.148×10^{-13}	-1.319×10^{-8}	5.119×10^{-4}	4.797	0.99237
$T = 45$ °C		1.168×10^{-11}	-2.283×10^{-7}	1.946×10^{-3}	3.826	0.99052
$T = 50$ °C		7.298×10^{-11}	-4.780×10^{-7}	3.528×10^{-3}	5.248	0.99127
$T = 55$ °C		6.103×10^{-9}	-1.660×10^{-5}	1.806×10^{-2}	3.663	0.99529
$T = 60$ °C		3.911×10^{-7}	-2.183×10^{-4}	6.091×10^{-2}	3.000	0.99683

Stereoscan 200 and the acceleration voltage used was 20 kV. Prior to examination, the surfaces were sputtered with gold.

2.3. Creep crack propagation tests

SENT specimens were tested under creep conditions by applying a constant tensile load, P, of 1200 N using an Instron 4502 test machine equipped with a thermostatic chamber (Instron model 3119). Creep crack growth was evaluated at various temperatures in the range between 32 and 60 °C. The crack length during creep tests was monitored by using the same system (video-camera and video-recorder) used for the FCP tests.

The applied stress intensity factor, K, was evaluated by Eq. (4) where P instead of ΔP was considered. The crack velocity da/dt was evaluated by interpolating the crack length versus time curves with a best fitting third order polynomial function (Table 1) [19].

2.4. Tensile tests

Uniaxial tensile tests were performed on rectangular unnotched specimens of $27 \times 120 \times 2.7$ mm^3 at a cross-head speed of 1 mm/min using an Instron 4502 test machine equipped with a 10 kN load cell. Use of a thermostatic chamber (Instron model 3119) enabled test to be carried out over a range of temperature. The yield stress was evaluated as the zero slope point on the stress–strain curves of at least three specimens.

3. Results and discussion

3.1. Fatigue crack propagation

During FCP experiments the crack advance is characterized by some damage and branching, but in any case a ‘prevalent crack’ can always be detected so that the failure behaviour of the material is mainly governed by this ‘prevalent crack’, with all other damage processes (including branching) of secondary importance. The appearance of the fracture surfaces of specimens failed after FCP test are similar and independent of the test frequency. A photograph

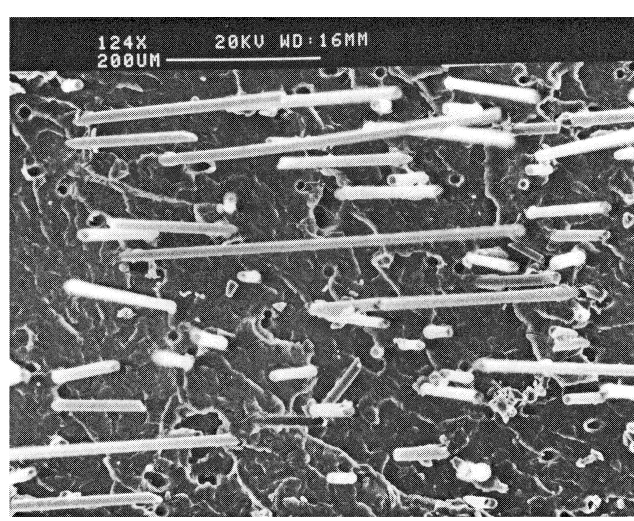

Fig. 2. Scanning electron microscope (SEM) picture of the fatigue fracture surface of iPP reinforced by 10 wt% of coupled glass fibers.

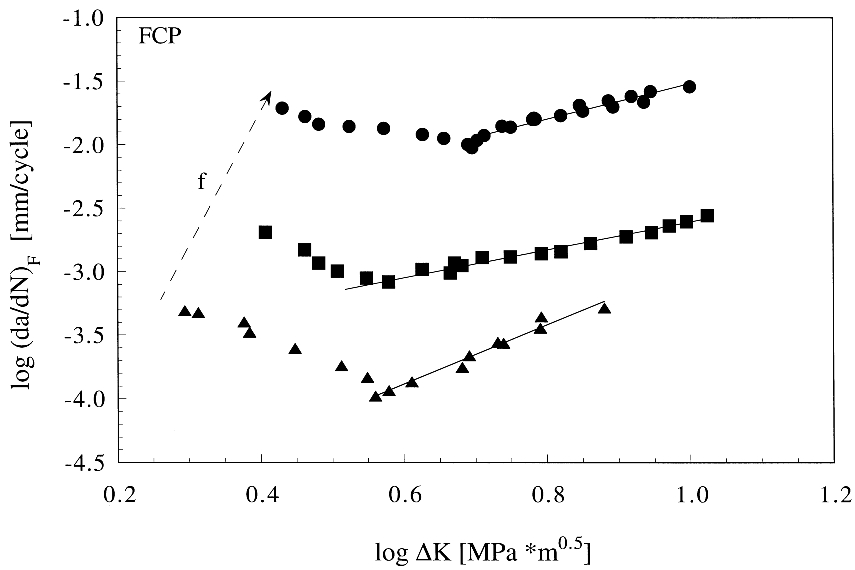

Fig. 3. Total crack propagation rate, $(da/dN)_F$, as a function of the stress intensity factor amplitude, ΔK, during FCP tests at various frequencies, f, i.e. (●) 0.1 Hz, (■) 1 Hz, and (▲) 10 Hz.

of the characteristic appearance of the fracture surface of a fatigue cracked specimen is shown in Fig. 2. It is interesting to observe that the fracture surface appears relatively smooth, showing a number of debonded fibers.

FCP data are shown in Fig. 3 as a log–log plot of crack growth rate da/dN as a function of the stress intensity factor amplitude for three different test frequencies (0.1, 1, 10 Hz). As already reported in the literature [5–10,20] the FCP behaviour of short-glass fibre reinforced polypropylene is characterised by an initial region where crack deceleration occurs with increasing crack length. By microscopic examination on unfilled iPP during fatigue test, Chudnovsky et al. [20] observed that crazes (damage) disseminate around and ahead of the main crack thus controlling its rate of propagation. More recently Karger-Kocsis [6,7] pointed out that during fatigue cycling the notch tip is probably subjected to a blunting phenomenon which could account for the observed FCP rate decrease. The minimum value of the FCP rate has been associated with the development of a damaged zone characterised by a critical damage density [7]. This point corresponds to the onset of a stable crack propagation range usually described by the Paris–Erdogan relationship represented by Eq. (1). From Fig. 3 it clearly emerges that the FCP resistance of the material under investigation is strongly influenced by the frequency of the fatigue load. In particular, the lower the frequency the higher the FCP rate at any ΔK value during fatigue experiments. The FCP data in the stable crack propagation range have been analysed following the approach proposed by Hertzberg et al. [13] who suggested that the overall crack

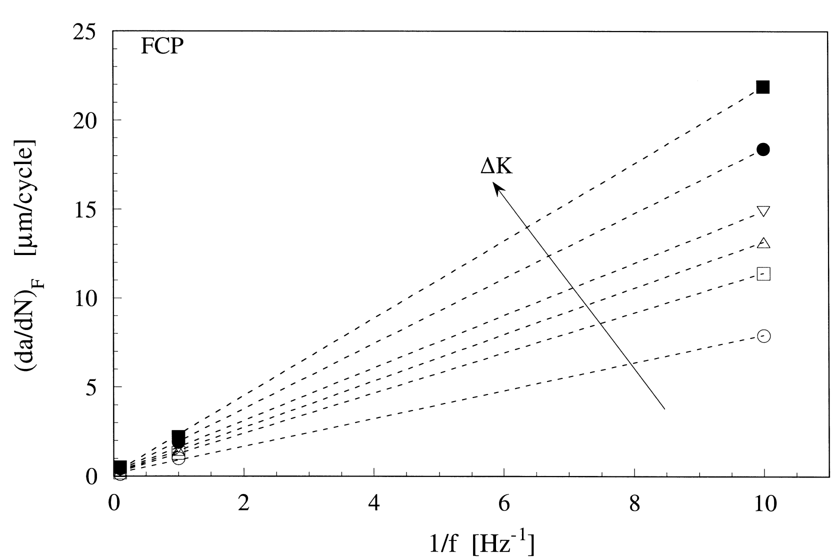

Fig. 4. Total crack propagation rate, $(da/dN)_F$, as a function of the time period, $1/f$, during FCP tests at various stress intensity factor amplitudes, i.e. (○) 4 MPa m$^{1/2}$, (□) 5 MPa m$^{1/2}$, (△) 5.5 MPa m$^{1/2}$, (▽) 6 MPa m$^{1/2}$, (●) 7 MPa m$^{1/2}$, (■) 8 MPa m$^{1/2}$.

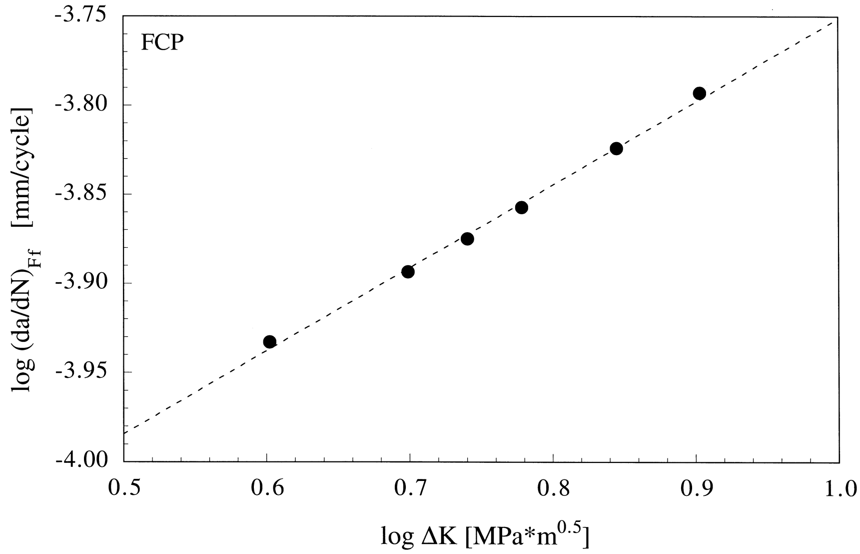

Fig. 5. Pure fatigue component, $(da/dN)_{Ff}$, as a function of the stress intensity factor amplitude, ΔK, during FCP tests.

extension rate during FCP, $(da/dN)_F$, could be considered as composed of two terms, i.e. pure fatigue component, $(da/dN)_{Ff}$, and a pure creep component $(da/dN)_{Fc}$, as indicated in the following equation:

$$\left(\frac{da}{dN}\right)_F = \left(\frac{da}{dN}\right)_{Ff} + \left(\frac{da}{dN}\right)_{Fc} \tag{5}$$

Wyzgoski et al. [14] proposed to rearrange Eq. (5) in the following form:

$$\left(\frac{da}{dN}\right)_F = \left(\frac{da}{dN}\right)_{Ff} + \left(\frac{da}{dt}\right)_{Fc} \frac{dt}{dN} \tag{6}$$

By considering that dt/dN is the time period of the cyclic oscillation, which is also equal to the inverse of the frequency, Eq. (6) can also be written as

$$\left(\frac{da}{dN}\right)_F = \left(\frac{da}{dN}\right)_{Ff} + \left(\frac{da}{dt}\right)_{Fc} \frac{1}{f} \tag{7}$$

where f is the test frequency.

The linear relationship existing between the total FCP rate per cycle and $1/f$ is evident in Fig. 4, for various levels of stress intensity factor amplitude reached in the stable crack acceleration region. It is worth nothing that according to Eq. (7), for any given ΔK value, the slope of the linear regression line in Fig. 4 represents the crack growth velocity contribution due to viscoelastic creep while the intercept with the axis of ordinates represents the crack growth rate component related to pure fatigue. On a log–log plot this latter component increases linearly with ΔK as shown in Fig. 5, which can hence be considered as a Paris plot for

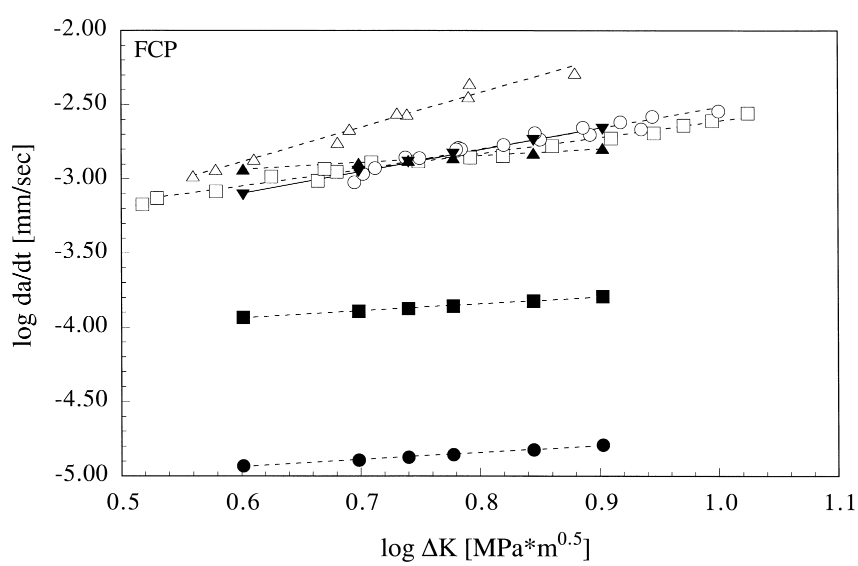

Fig. 6. Total crack velocity, $(da/dt)_F$, during FCP tests at (○) 0.1 Hz, (□) 1 Hz, and (△) 10 Hz compared with the calculated (▼) pure creep component, $(da/dt)_{Fc}$, and pure fatigue components, $(da/dt)_{Ff}$, at (●) 0.1 Hz, (■) 1 Hz, and (▲) 10 Hz.

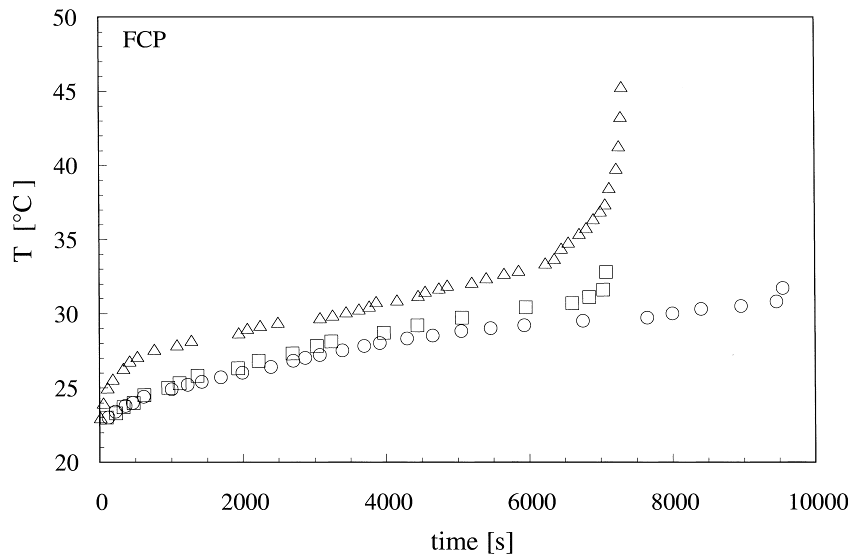

Fig. 7. Temperature measured on the specimen surface near the crack tip during FCP experiments at (○) 0.1 Hz, (□) 1 Hz, and (△) 10 Hz.

the pure FCP component. On the basis of the information reported in Fig. 5 it is now possible to separate and estimate the components of the fatigue and CCP velocities within the data in Fig. 3. The separated data are shown in Fig. 6; the pure creep crack velocity component is independent of frequency while the pure fatigue crack growth depends linearly on the test frequency, being $(\mathrm{d}a/\mathrm{d}N)_{\mathrm{Ff}} = (\mathrm{d}a/\mathrm{d}t)_{\mathrm{Ff}} \times (1/f)$. It is interesting to observe that during the FCP experiments at low frequencies (0.1 and 1 Hz) crack propagation mainly occurs by viscoelastic creep since the pure fatigue crack velocity components are one to two orders of magnitude lower than the pure creep crack velocity. At higher frequency (10 Hz) the creep and fatigue crack components are of similar magnitude.

The temperature measurements on the specimen surface near the crack tip zone made by the infrared camera indicated that a hysteretic heating occurs. As shown in Fig. 7 the crack tip temperature is characterised by a trend which quite rapidly increases during the initial stages, steadily increases during the stable FCP propagation, and abruptly increases when the specimen is approaching fracture instability. The intensity of this temperature increase is more pronounced as the test frequency increases.

3.2. Creep crack propagation

Crack extension, Δa, versus loading time during CCP experiments at various temperatures are reported in Fig. 8. The similarity of the fracture kinetics at different temperatures clearly appears, the effect of increasing temperature consisting substantially in a shortening of the whole fracture process. The kinetics of crack propagation under creep

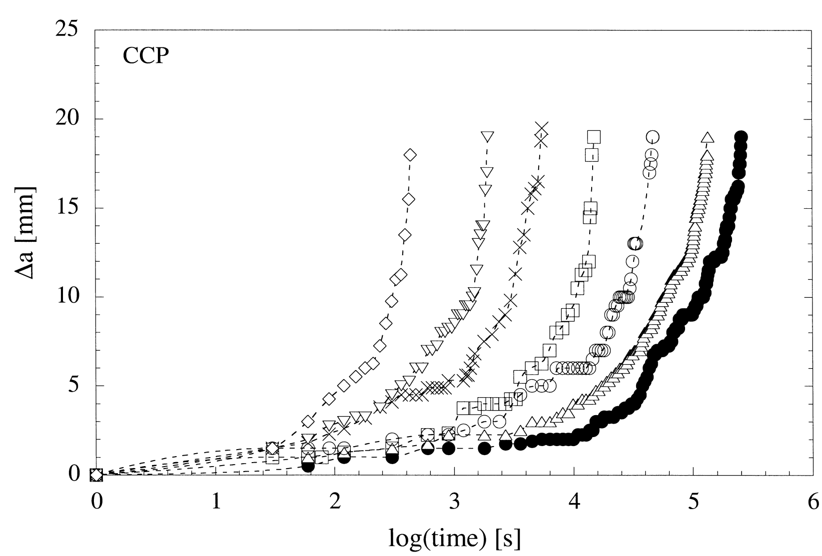

Fig. 8. Crack length increment, Δa, versus time for CCP tests performed at various temperatures. Symbols refer to (●) 32 °C, (△) 35 °C, (○) 40 °C, (□) 45 °C, (×) 50 °C, (▽) 55 °C, and (◇) 60 °C.

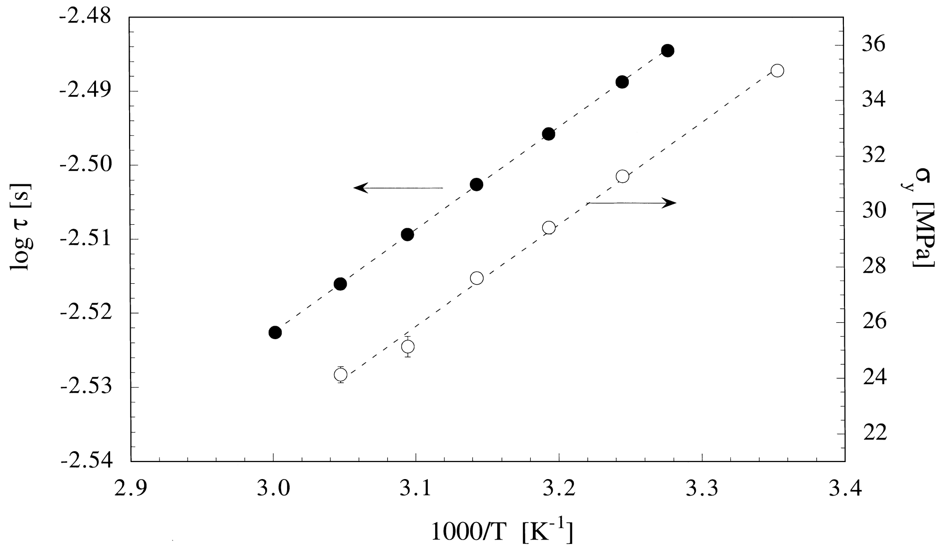

Fig. 9. Temperature dependence of the time to failure, τ, in CCP experiments (●), and of the yield stress, σ_y, in tensile tests (○).

condition is extremely sensitive to test temperature. In fact it is well known that for many different materials, including plastics, the lifetime, τ, depends on the absolute temperature, T, through a relationship in the form [21]

$$\tau = \tau_0 \exp\left[\frac{(U_0 - \gamma\sigma)}{kT}\right] \tag{8}$$

where k is the Boltzman's constant, σ is the applied stress; τ_0, U_0 and γ are material constants. In our case, experimental data are in good accordance with Eq. (8) as shown by the linear relationship between the logarithm of the time to failure and the inverse of the absolute temperature, Fig. 9. The model leading to Eq. (8) is based on the gradual exhaustion of the load-bearing capability of the polymer through time-dependent breakage of primary bonds or polymer chains (molecular approach) [22]. In general, creep rupture of a polymer is a result of various events like viscoelastic deformation, primary and secondary bond failure, and yielding [23]. In the present case yielding seems to play a major role, as the yield stress of the composite is strongly dependent on temperature in the range of interest, see Fig. 9.

Crack length versus time curves (Fig. 8) have been interpolated with a best fitting third order polynomial function in order to evaluate a CCP velocity, $(da/dt)_C$, which is plotted in Fig. 10 as a function of the applied stress intensity factor on a log–log plot. It is interesting to observe that CCP strongly resemble FCP behaviour, with the crack velocity initially decreasing to a minimum value and then steadily increasing up to final failure. The crack deceleration observed during CCP experiments could be very likely due to a blunting process localized at the crack tip, as discussed

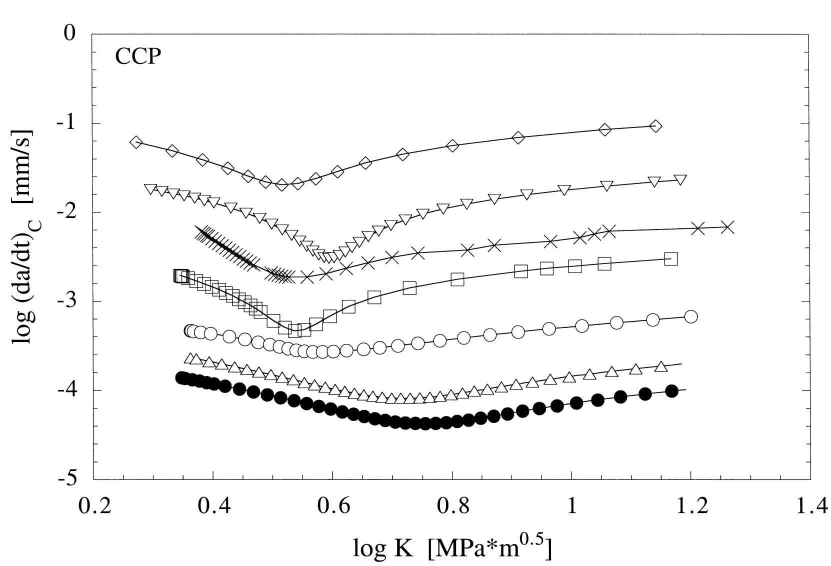

Fig. 10. Crack velocity $(da/dt)_C$ versus the stress intensity factor for CCP tests performed at various temperatures. Symbols refer to (●) 32 °C, (△) 35 °C, (○) 40 °C, (□) 45 °C, (×) 50 °C, (▽) 55 °C, and (◇) 60 °C.

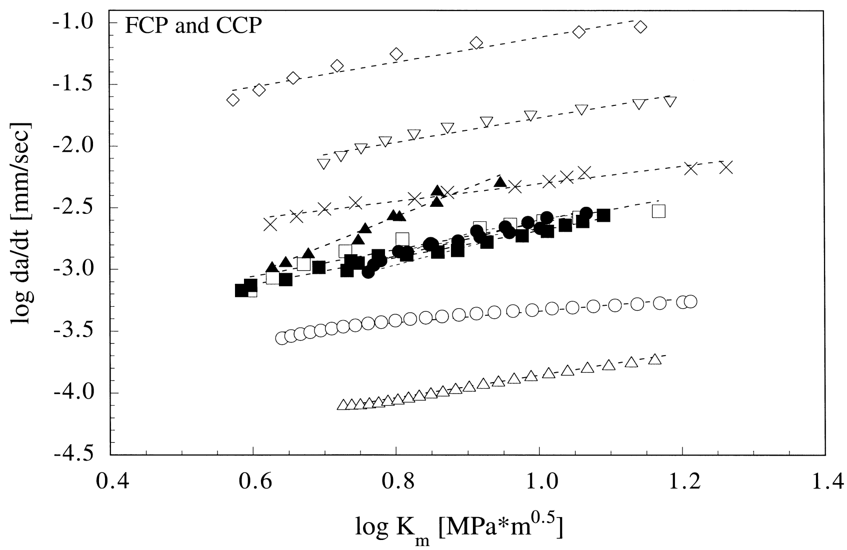

Fig. 11. Comparison between total crack velocity versus mean stress intensity factor in the stable acceleration range for FCP tests performed at (●) 0.1 Hz, (■) 1 Hz, and (▲) 10 Hz, and CCP tests performed at various temperatures (△) 35 °C, (○) 40 °C, (□) 45 °C, (×) 50 °C, (▽) 55 °C, and (◇) 60 °C.

for the FCP tests. In order to compare FCP and CCP data it is convenient to define a mean applied stress intensity factor for the FCP tests, K_m, which is related to ΔK through the following relationship

$$K_m = \frac{1+R}{2(1-R)}\Delta K \quad (9)$$

where R is the minimum to maximum load ratio.

Of course for CCP test K_m is equal to the applied stress intensity factor K. Fatigue and creep crack velocities in the stable crack acceleration region can now be compared as shown in Fig. 11. The results obtained for the exponential (m and n) and pre-exponential (A' and B) terms of Eqs. (2) and (3) are summarized in Table 2. It is worth noting that FCP lines at 0.1 and 1 Hz are characterised by a slopes of about 1.4 and 1.1, respectively, which are only slightly higher than the average slope of the CCP lines (about 0.9 ± 0.2). It can observed that FCP at low frequencies (0.1 and 1 Hz) are substantially equivalent to an isothermal CCP at 45 °C. It is well known that temperature during FCP is not uniformly distributed in the specimen cross-section and it has a peak at the crack tip [14,15,24]. Consequently such a temperature level cannot strictly be considered the actual temperature of the specimen during FCP, but it can reasonably represents an equivalent mean temperature at which FCP occurs at 0.1 and 1 Hz. Moreover, it is worthwhile to observe that this temperature level is considerably higher than that measured by the infrared analysis of the specimen surface during FCP which spans from about 26 to 30 °C in the stable crack acceleration region. At higher frequency (10 Hz) FCP data line is characterised by a slope much steeper (about 2.3) than the CCP line. This behaviour could be related to the presence of a higher pure fatigue component, as already evidenced in Section 3.1, as well as to a stronger non-isothermal character of the crack propagation. It should be recognized that a change in the test frequency alters the number of loading cycles per unit time and the integrated time under load for each load excursion. It is thus reasonable to suppose that the higher creep component evidenced for low frequency tests could be mostly attributed to the higher time under load during FCP experiments. The existence of a creep crack growth contribution during FCP tests markedly dependent on the time-under-load has been confirmed by various FCP experiment conducted with different loading waveforms [15].

Table 2
Pre-exponential (A' and B) and exponential (m and n) terms of Eqs. (2) and (3)

FCP data	$\log A'\left[\frac{\text{mm/s}}{(\text{MPa m}^{1/2})^m}\right]$	m
$f = 0.1$ Hz	−4.0182	1.4059
$f = 1$ Hz	−3.7838	1.0996
$f = 10$ Hz	−4.4419	2.3330
CCP data	$\log B\left[\frac{\text{mm/s}}{\text{MPa m}^{1/2})^n}\right]$	n
$T = 32$ °C	−5.1157	0.9553
$T = 35$ °C	−4.7667	0.9097
$T = 40$ °C	−3.8250	0.4897
$T = 45$ °C	−3.7074	1.0837
$T = 50$ °C	−3.0229	0.7162
$T = 55$ °C	−2.7699	0.9952
$T = 60$ °C	−2.1251	1.0058

4. Conclusions

On the basis of the results obtained in the present work, it can be concluded that in iPP reinforced with short E-glass fibres under cyclic loading at a positive mean stress, creep crack growth contribution can be the governing effect in material failure, depending on test frequency. This effect, qualitatively reported by the authors in previous works [8–10] has been quantitatively assessed here. In particular, it has been found that at low frequencies (0. 1 and 1 Hz) the role of creep is predominant, creep crack being at least one order of magnitude higher than the pure fatigue component. At these frequency levels, the crack growth process can be considered as equivalent to an isothermal creep crack growth at a temperature much higher (up to 20 °C) than the test temperature (room temperature). At higher frequency (10 Hz) creep and fatigue crack growth becomes comparable giving about the same contribution to the overall crack. The higher creep component evidenced for low frequency tests could be mostly attributed to the higher time under load during FCP experiments.

Acknowledgements

This work was partially supported by Consiglio Nazionale delle Ricerche, CNR, Rome. Montell Polyolefins SpA (now Basell Poliolefine Italia S.p.A.), Ferrara, Italy, is kindly acknowledged for the provision of the materials. The authors would like to thank Mr A. Dimauro for his contribution to the experimental work.

References

[1] Bernreiter K, Hammerschmid K. Designing properties of polypropylene. In: Karger-Kocsis J, editor. Polypropylene: an A–Z reference. London: Kluwer; 1999. p. 148–57.

[2] Song J, Prox M, Weber A, Ehrenstein GW. Self-reinforcement of polypropylene. In: Karger-Kocsis J, editor. Polypropylene: structure, blends and composites. Structure and morphology, vol. 1. London: Chapman & Hall; 1995. p. 142–201.

[3] Pukanszky B. Particulate filled polypropylene. In: Karger-Kocsis J, editor. Polypropylene: structure, blends and composites. Composites, vol. 3. London: Chapman & Hall; 1995. p. 1–70.

[4] Gibson AG. Processing and properties of reinforced polypropylenes. In: Karger-Kocsis J, editor. Polypropylene: structure, blends and composites. Composites, vol. 3. London: Chapman & Hall; 1995. p. 71–112.

[5] Karger-Kocsis J. Microstructural aspects of fracture in polypropylene and its filled, chopped fibre and fibre mat reinforced composites. In: Karger-Kocsis J, editor. Polypropylene: structure, blends and composites. Composites, vol. 3. London: Chapman & Hall; 1995. p. 142–201.

[6] Karger-Kocsis J, Friedrich K. Effect of skin–core morphology on fatigue crack propagation in injection moulded polypropylene homopolymer. Int J Fatig 1989;11:161–8.

[7] Karger-Kocsis J, Friedrich K, Bailey RS. Fatigue crack propagation in short and long glass fiber reinforced injection-molded polypropylene composites. Adv Compos Mater 1991;1:103–21.

[8] Pegoretti K, Ricco T. Fatigue behaviour of fiber reinforced polypropylene. Proceedings of ECCM-8 Conference, Naples; June 1998. p. 135–42.

[9] Pegoretti A, Ricco T. Fatigue crack propagation in polypropylene reinforced with short glass fibres. Compos Sci Technol 1999;59: 1055–62.

[10] Pegoretti A, Ricco T. Fatigue fracture of neat and short glass fiber reinforced polypropylene: effect of frequency and material orientation. J Compos Mater 2000;34(12):1009–27.

[11] Paris PC, Erdogan F. A critical analysis of crack propagation laws. J Basic Engng Trans 1963;85:528–37.

[12] Karger-Kocsis J. Fatigue performance of polypropylene and related composites. In: Karger-Kocsis J, editor. Polypropylene: an A–Z reference. London: Kluwer; 1999. p. 227–32.

[13] Hertzberg RW, Manson JA, Skibo MD. Frequency sensitivity of fatigue processes in polymeric solids. Polym Engng Sci 1975;15: 252–60.

[14] Wyzgoski MG, Novak GE, Simon DL. Fatigue and fracture of nylon polymers. Part 1. Effect of frequency. J Mater Sci 1990;25: 4501–10.

[15] Hertzberg RW, Manson JA. Fatigue of engineering plastics. New York: Academic Press; 1980. p. 74–141.

[16] Parsons M, Stepanov EV, Hiltner A, Baer E. Correlation of stepwise fatigue and creep slow crack growth in high density polyethylene. J Mater Sci 1999;34:3315–26.

[17] Parsons M, Stepanov EV, Hiltner A, Baer E. Correlation of fatigue and creep slow crack growth in medium density polyethylene pipe material. J Mater Sci 2000;35:2659–74.

[18] Broek D. Elementary engineering fracture mechanics. Dordrecht: Martinus Nijhoff Publishers; 1987. p. 85.

[19] Pegoretti A, Ricco T. Creep crack growth in a short glass fibres reinforced polypropylene composite. J Mater Sci 2001;36:4637–41.

[20] Chudnovsky A, Moet A, Bankert RJ, Takemori MT. Effect of damage dissemination on crack propagation in polypropylene. J Appl Phys 1983;54:5562–7.

[21] Zhurkov SN. Kinetics concept of the strength of solids. Int J Fract Mech 1965;1:311–23.

[22] Raghavan J, Meshii M. Creep rupture of polymer composites. Compos Sci Technol 1997;57:375–88.

[23] Jayaraman R. Fracture criteria to predict creep rupture. Trends Polym Sci 1997;5:116–22.

[24] Lang RW, Manson JA. Crack tip heating in short-fibre composites under fatigue loading conditions. J Mater Sci 1987;22:3576–80.